Hindawi
Journal of Nanomaterials
Volume 2018, Article ID 6845026, 11 pages
https://doi.org/10.1155/2018/6845026

Research Article

Facile Synthesis of Tin Oxide Hollow Nanoflowers Interfering with Quorum Sensing-Regulated Functions and Bacterial Biofilms

Nasser A. Al-Shabib,[1] **Fohad Mabood Husain**,[1] **Naushad Ahmad**,[2] **Faizan Abul Qais**,[3] **Aslam Khan**,[4] **Altaf Khan**,[5] **Mohammad Shavez Khan**,[3] **Javed Masood Khan**,[1] **Syed Ali Shahzad**,[1] **and Iqbal Ahmad**[3]

[1]*Department of Food Science and Nutrition, College of Food and Agriculture, King Saud University, Riyadh 11451, Saudi Arabia*
[2]*Department of Chemistry, College of Science, King Saud University, Riyadh 11451, Saudi Arabia*
[3]*Department of Agricultural Microbiology, Aligarh Muslim University, Aligarh 202002, India*
[4]*King Abdullah Institute for Nanotechnology, King Saud University, Riyadh 11451, Saudi Arabia*
[5]*Department of Pharmacology, Central Research Laboratory, Microbiology Unit, College of Pharmacy, King Saud University, Riyadh 11451, Saudi Arabia*

Correspondence should be addressed to Nasser A. Al-Shabib; nalshabib@ksu.edu.sa
and Fohad Mabood Husain; fahadamu@gmail.com

Received 1 September 2018; Accepted 31 October 2018; Published 6 December 2018

Academic Editor: Vincenzo Baglio

Monophasic tin dioxide nanoflowers (TONFs) assembled by rod-like nanostructures were prepared by coprecipitation method using tin chloride and ammonia precipitators, as the starting materials, without using any surfactants or templates. The structural, compositional, optical, and morphological properties of TONFs were investigated by XRD, FT-IR, UV-vis, SEM-EDX, and TEM techniques. Synthesized TONFs demonstrated inhibition of quorum sensing- (QS-) regulated virulence in pathogens, viz., *Chromobacterium violaceum*, *Pseudomonas aeruginosa*, and *Serratia marcescens*. Significant reduction in biofilm formation in all test pathogens was also observed which was further validated by CLSM images illustrating disturbed biofilm architecture. Vital functions like EPS, swarming motility, and cell surface hydrophobicity that contribute to successful biofilm formation were reduced after addition of sub-MICs of TONFs. Significant eradication of preformed biofilms was recorded upon addition of subinhibitory concentrations of TONFs in all test pathogens. The study highlights the broad-spectrum QS and biofilm inhibition by TONFs that can be exploited in future to protect food from contamination and combatting persistent drug-resistant infections.

1. Introduction

The food industry is encountering excessive economic losses due to the spoilage and contamination of food products by microbes [1]. This spoilage of food is often linked to a density-dependent cell-cell communication system quorum sensing (QS). Communication is intra- as well as interspecies both in Gram-positive and in Gram-negative bacteria. Bacteria communicate and coordinate their behavior when they achieve an optimum population density and produce signaling molecules called autoinducers [2, 3]. Autoinducers (AIs) coordinate the production of various phenotypic and physiological characteristics. Acyl-homoserine lactones (AHLs), autoinducer peptides (AIPs), and autoinducer-2 (AI-2s) molecules are the three major classes of AIs [4]. These AIs regulate various enzymatic activities and siderophore-mediated iron chelation, which are associated with food spoilage [5]. In Gram-negative bacteria, AHL-based QS regulates the production of violacein pigment (*Chromobacterium violaceum*), virulence factors (*Pseudomonas aeruginosa*), flagellar motility (*Listeria monocytogenes*), bioluminescence in *Vibrio harveyi* and *Vibrio fischeri*, sporulation, and development of mature biofilms through cell differentiation and community organization

[6, 7]. Various reports pertaining to food spoilage have demonstrated the role of QS in biofilm formation in food. Biofilm is a complex aggregation of the bacterial population with protected proliferation enabling them to stay alive in hostile environments as in human host [8–10]. Additionally, it enables them to disperse and colonize by the formation of biofilms [11]. Biofilm formation has been reported to be associated with more than 80% of infections caused by pathogenic bacteria. Therefore, biofilms can be considered as a special mode of persistent bacterial infection.

In recent past, extensive investigations on safe food preservatives have been carried out and QS in bacteria has emerged as an attractive target [12–15]. Nanostructured materials due to their peculiar physical and chemical properties have caught the eye of the scientific community. It has potentially influenced the food packaging industry to a great extent as nanomaterials show improved flexibility, gas barrier properties, temperature and moisture stability, etc. Further, incorporation and integration of active antimicrobial, oxygen-scavenging agents, antioxidants, and intelligent nanosensors for monitoring the condition of food are expected to provide advanced packaging solutions [16, 17]. Metallic nanoparticles and their oxides are being exploited in almost all sectors due to the development of rapid and economical methods of synthesis. Moreover, the material is found to be safe, nontoxic, and stable [18, 19].

Tin oxide nanoparticles (TONPs) are one of the important materials that have been exploited widely to reduce air pollution and in the detection of toxic/smelling gases at low levels in the air as well as at industrial and domestic levels [20]. Owing to their antimicrobial and antioxidant properties, tin oxide nanoparticles are deemed to be excellent candidates for biomedical applications [21–23]. Although antimicrobial properties of tin oxide nanoparticles are well documented, very little data is available on the effect of nanoparticles with special reference to nano tin on QS-controlled virulence and biofilm.

Therefore, the present investigation reports facile synthesis and characterization of SnO_2 hollow nanoflowers composed of small nanorods. The prepared SnO_2-NFs were examined regarding their morphological and structural properties using X-ray diffraction (XRD) spectroscopy, Fourier transform infrared spectroscopy (FT-IR), UV-vis diffuse reflectance spectroscopy, scanning electron microscopy (SEM), and transmission electron microscopy (TEM). We have assessed the ability of these nanoflowers to interfere with QS-regulated virulence functions in test pathogenic bacteria. Further, we examined the effect of synthesized nanoparticles on biofilm formation and on the eradication of preformed biofilms. To the best of our knowledge, this is the first report on tin oxide nanoparticles demonstrating the inhibition of QS-controlled functions with special reference to biofilm.

2. Materials and Methods

Tin(IV) chloride ($SnCl_4{\cdot}xH_2O$) used as the precursor for the synthesis of tin oxide NPs and ammonia solution (NH_4OH) were purchased from Sigma-Aldrich. All solutions were prepared using deionized water.

2.1. Synthesis of SnO_2 Nanoflowers (TONFs). SnO_2-NFs were synthesized by a facile, economic, and surfactant-/template-free precipitation method. Briefly, 3.47 cm^3 $SnCl_4$ was dissolved in 200 cm^3 ethanol and stirred for 30 min till a transparent solution was obtained. The ammonia solution (NH4OH) was dropped to the starting solution under stirring to keep a constant pH value (pH = 8). The solution was put under an ultrasonic wave apparatus for 30 min to obtain homogenous solution which was then aged for 12 h. The black precipitate was collected by filtration then washed by distilled water and ethanol for three times. After drying at 85°C for 4 h in the oven, the precursor was calcined at 600°C for 3 h. After cooling, tin oxide nanoparticles were obtained.

2.2. Characterization of TONFs. The phase and crystal structure of the products was determined by powder X-ray diffractometer (Ultima IV Rigaku with Cu Kα radiation). FTIR spectra of the sample were recorded on a Thermo Nicolet 380 USA spectrometer using a KBr pellet technique in the range of 4000-400 cm^{-1}. The pellets were made of a mixture of 100 mg KBr dried at 120°C and 2 mg of the studied sample. UV-vis absorption spectra of the synthesized nanoparticles were obtained using a UV-vis spectrophotometer (Shimadzu UV-1800, Japan). Transmission electron microscopy (TEM) (JEOL 2100) was operated at 200 kV, and the morphological and elemental compositions of SnO_2 NPs were studied by scanning electron microscopy (SEM) on a JEOL FE-SEM (JSM 7600F) microscope-coupled energy-dispersive spectroscopy (Oxford) analysis system.

2.3. Bacterial Strains. Bacterial strains used in the present investigation were *Chromobacterium violaceum* ATCC 12472, *Pseudomonas aeruginosa* PAO1, *Serratia marcescens* ATCC 13880, and *Listeria monocytogenes* (laboratory strain). All bacteria were cultivated on Luria-Bertani (LB) medium. *P. aeruginosa* and *L. monocytogenes* were grown at 37°C while *C. violaceum* and *S. marcescens* were cultivated at 30°C.

2.4. Determination of Minimum Inhibitory Concentration (MIC). Minimum inhibitory concentrations of synthesized TONFs against the bacterial pathogens were determined using the 96-well plate microbroth dilution method described by Klančnik et al. [24]. The minimum concentration of tin nanoflowers at which there was no visible growth of bacteria was recorded as MIC. Concentrations lower than MICs were used to study the effect of synthesized nanoflowers on QS and biofilm in pathogenic bacteria.

2.5. Violacein Inhibition Assay. Violacein production by biosensor strain *C. violaceum* ATCC 12472 (CV12472) in the presence of subinhibitory concentrations of TONFs was studied using the method described by Husain et al. [25]. Briefly, CV12472 was incubated overnight and transferred to Erlenmeyer flasks containing Luria broth (LB) supplemented with 2-16 μg/ml concentrations of TONFs. All flasks were incubated for 24 h in a shaking incubator. 1 ml of incubated culture was centrifuged for 10 min, and 1 ml of DMSO was added to the resultant pellet. This solution was vortexed vigorously for 30 seconds and centrifuged at

13000 rev/min for 10 min to remove the cells. The resultant supernatant (200 μl) was added to 96-well flat-bottomed microplates (NunC), and absorbance was read at 585 nm. Observations were measured in terms of % inhibition using the following formulae:

$$\%\text{Reduction} = \left[\frac{(\text{OD585control} - \text{OD585sample})}{\text{O}}\,\text{D585control}\right] \times 100. \quad (1)$$

2.6. Virulence Assays in P. aeruginosa. The effect of sub-MICs of TONFs on the production of QS-regulated virulence factors, namely, LasB elastase, protease, pyocyanin, and alginate, was determined by employing methods described previously [26, 27].

2.7. Prodigiosin Assay in S. marcescens. Overnight grown *S. marcescens* (1%) was inoculated into 2 ml of fresh LB supplemented with sub-MICs of TONFs. Late stationary phase cells were collected and centrifuged for 10 min at 10000 rpm. Prodigiosin from the pellet was extracted with acidified ethanol solution, and absorbance was measured at 534 nm [28].

2.8. Biofilm Inhibition. Biofilm inhibition by TONFs was determined using the method described by Kalishwaralal et al. [29]. Briefly, test pathogens grown overnight were reinoculated in fresh LB medium with or without subinhibitory concentrations of TONFs and incubated at 37°C for 24 h. Biofilms formed in microtitre plates were washed with PBS, stained with a 0.1% crystal violet solution, and quantified by measuring the absorbance at OD_{595}.

2.9. Extraction and Quantification of Exopolysaccharide (EPS). Pathogens under study were cultivated with or without sub-MICs of TONFs and centrifuged. The resulting supernatant was filtered, and three volumes of chilled 100% ethanol were added to it. The supernatant-ethanol mixture was incubated for 18 h at 4°C to precipitate out the EPS [30]. The Dubois method of estimating sugars was used to compute the EPS production [31].

2.10. Swarming Motility Assay. Overnight culture of the test pathogens was point-inoculated at the center of LB medium plates consisting of 0.3% agar with or without various subinhibitory concentrations of TONFs [32].

2.11. Cell Surface Hydrophobicity Assay. Cell surface hydrophobicity (CSH) was determined using the protocol described by Viszwapriya et al. [33]. Pathogens (1 ml) grown overnight in the presence and absence of TONFs were mixed with 1 ml of toluene and vortexed for 2 min. To facilitate phase separation, these tubes were left undisturbed for 15 min. Bacterial density of the aqueous phase was measured at 600 nm. Percent (%) CSH was determined by using the following equation: $[1 - (\text{OD600 nm after vortexing}/\text{OD600 nm before vortexing})] \times 100$.

2.12. Biofilm Eradication Assay. The effect of TONFs on preformed biofilms was assayed by growing the test bacteria in 96-well microtitre plates for 24 h at 37°C. After incubation, nonadhered cells were washed and wells were supplemented with fresh medium. 0.5 × MIC of TONFs were added to wells, and microtitre plates were incubated overnight. Wells of incubated plates were washed thrice with PBS and stained with 0.1% crystal violet. Eradication of preformed biofilm was quantified by measuring the absorbance at OD_{595} [34].

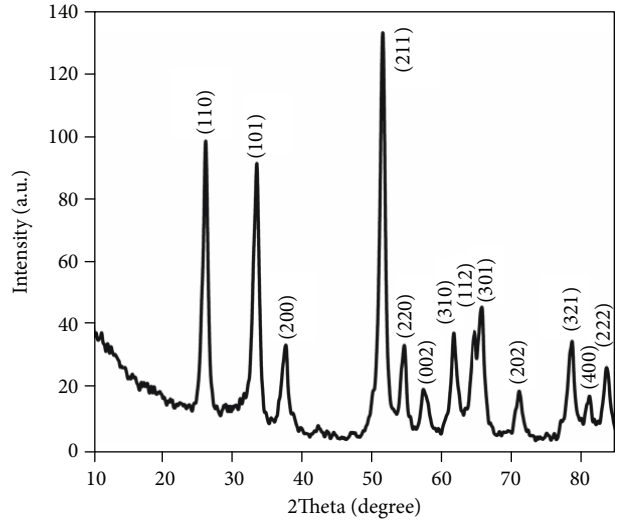

Figure 1: The XRD pattern of TONFs grown via the coprecipitation method.

3. Results and Discussion

3.1. XRD Analysis. Crystal structures and crystallinity of the synthesized SnO_2 powder were studied by X-ray diffraction (XRD), and the result is shown in Figure 1. The crystallinity of the sample is clearly evident by the sharper diffraction peaks at respective diffraction angles of the prepared SnO_2 powder. All of the peaks were matched with diffraction data of the tetragonal structure of tin oxide (JCPDS: 41-1445) and show a strong preferred orientation of (211) [35]. No other crystal phase is detected, indicating the high purity of the final product. Strong and sharp peaks indicate that the prepared product is highly crystalline. Tetragonal lattice parameters were found 0.492 nm for a and b and 0.328 nm for c, respectively. The major peaks of SnO_2 were located at $2\theta = 26.61°$, 33.93°, and 51.81°. The reflections are markedly broadened, which indicates that the crystallite size of SnO_2 nanoparticles is small. The crystallite size (D) determined from SnO_2 by the Scherrer formula is about 17.77 nm.

3.2. FTIR Spectra. The composition and quality of the product were analyzed by FTIR spectroscopy. Figure 2 shows the FTIR spectra of SnO_2 synthesized by the coprecipitation method. FTIR studies showed that chlorine contamination was completely removed by the washing process. The broad band around the 3390-3425 cm^{-1} region is due to the stretching vibration of the O–H bond. This band is due to the OH groups and the adsorbed water bound at the SnO_2 surface. The band at 1625–1635 cm^{-1} is attributed to the bending vibration of water molecules, trapped in the SnO_2 sample

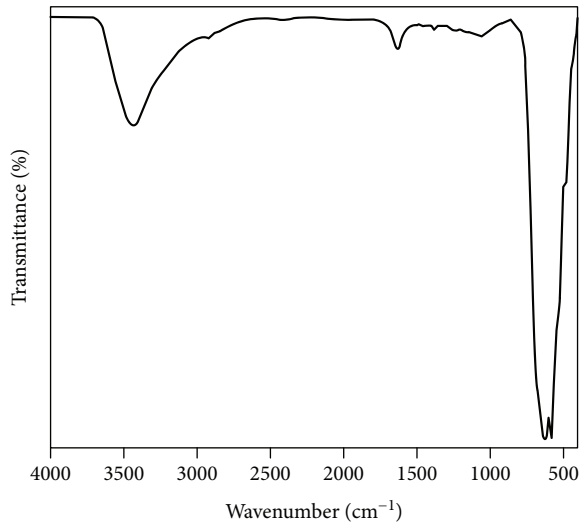

Figure 2: FT-IR spectra of TONFs.

[36]. The peak at 625 cm^{-1} agrees with the stretching modes of the Sn–O–Sn terminal Sn–OH, while the peak at the 580 cm^{-1} region corresponds to the stretching terminal of Sn–OH [37].

3.3. UV–Vis Analysis of TONFs. The optical properties of SnO_2 nanoparticles have been recorded by absorption spectra in the UV–visible wavelength range of 200–500 nm and are shown in Figure 3. Absorption was recorded at 285 nm, and this can be accredited to low coordination of surface oxide ion. This observation is because of the fact that as coordination decreases, the electrostatic potential of a O^{2-} ion in SnO_2 also decreases gradually, and thus, the whole process requires less energy.

The optical band gap energy (Eg) of SnO_2 nanoparticles is calculated from the equation given below [38]:

$$\alpha h\nu = A\left(h\nu - E_g\right)^n, \tag{2}$$

where α is the absorption coefficient, A is a constant, h is the Planck constant, and E_g is the band gap energy and n is equal to 1/2 and 2 for direct allowed transition and indirect allowed transition. The plot of $(\alpha h\nu)1/2$ versus $h\nu$ based on direct transition and gives absorption edge energy which is the band gap of the material, as is shown in the inset in Figure 3. The evaluated optical band gap energy of the SnO_2 nanoparticle is 3.98 eV which is larger than the value of 3.64 eV for bulk SnO_2 [39] because of the quantum confinement effect.

3.4. SEM and TEM Analysis. The scanning electron micrograph of SnO_2 nanoflowers is shown in Figure 4. The nanoparticles exhibited varied morphology, and the sizes are smaller than 50 nm (Figure 4(a)). Previously, nanocrystalline tin oxide (SnO_2) particles have been reported to exhibit uniform distribution grains with an average crystallite size of 52 nm [40]. In another finding, a controlled synthesis of monodispersed SnO_2 nanoparticles was found in which increasing pH from 6 to 9 resulted in decreased particle size

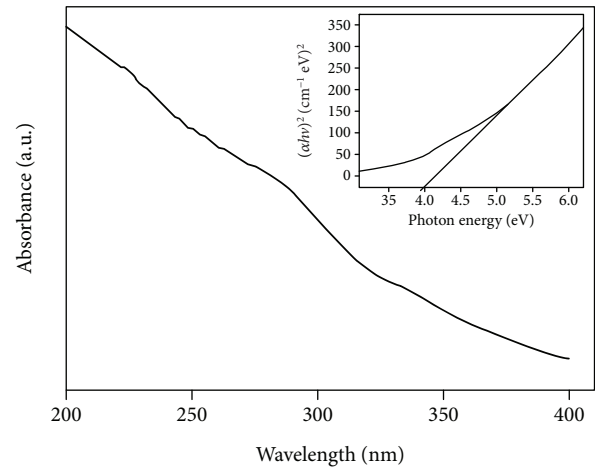

Figure 3: Optical absorption spectra of TONFs. Inset: a plot of $(\alpha h\nu)2$ versus photon energy (eV).

[41]. The energy-dispersive X-ray (EDX) spectrum of synthesized SnO_2 nanoparticles revealed the presence of tin and oxygen only. The composition of tin and oxygen by weight was 58.39 and 41.61%, respectively. The size distribution of nanoparticles depends on many factors during synthesis such as rate of nucleation, agglomeration, and growth processes [42].

Figure 5 shows the transmission electron micrographs of SnO_2 nanoflowers. The micrographs support the SEM findings of variation in shape and also validated the XRD results; here, the average particle size was found to be 17.77 nm. The shape of particles revealed by TEM was spheroidal along with anisotropies. Das et al. [43] reported the synthesis of nanorods and nanoparticles of SnO_2 using the solvothermal technique. The variation in shape and size of nanoparticles synthesized using different routes has also been reported earlier [44, 45].

3.5. Determination of MIC. MIC of TONFs was determined against pathogens *C. violaceum* 12472, *P. aeruginosa* PAO1, *L. monocytogenes*, and *S. marcescens*. MIC is the lowest concentration at which no visible growth of the test pathogen is observed, as depicted in Figure 6. MIC for TONFs against *P. aeruginosa* PAO1 and *S. marcescens* was found to be 128 μg/ml, while the lowest MIC of 32 μg/ml was recorded against CV12472. Further, minimum bactericidal concentration (MBC) was also assessed and is presented in Figure 6. MBC values for *C. violaceum* 12472, *P. aeruginosa* PAO1, *L. monocytogenes*, and *S. marcescens* were found to be 64, 256, 128, and 128 μg/ml, respectively. The effect of TONFs on quorum sensing-regulated functions and biofilm was assessed using sub-MICs (concentrations below MIC).

3.6. Effects of TONFs on Quorum Sensing-Regulated Functions

3.6.1. Violacein Inhibition in C. violaceum. QS inhibition by TONFs was assessed using *C. violaceum* 12472 indicated by the loss of purple pigmentation (violacein). TONFs reduced violacein production in CV12472 in a concentration-

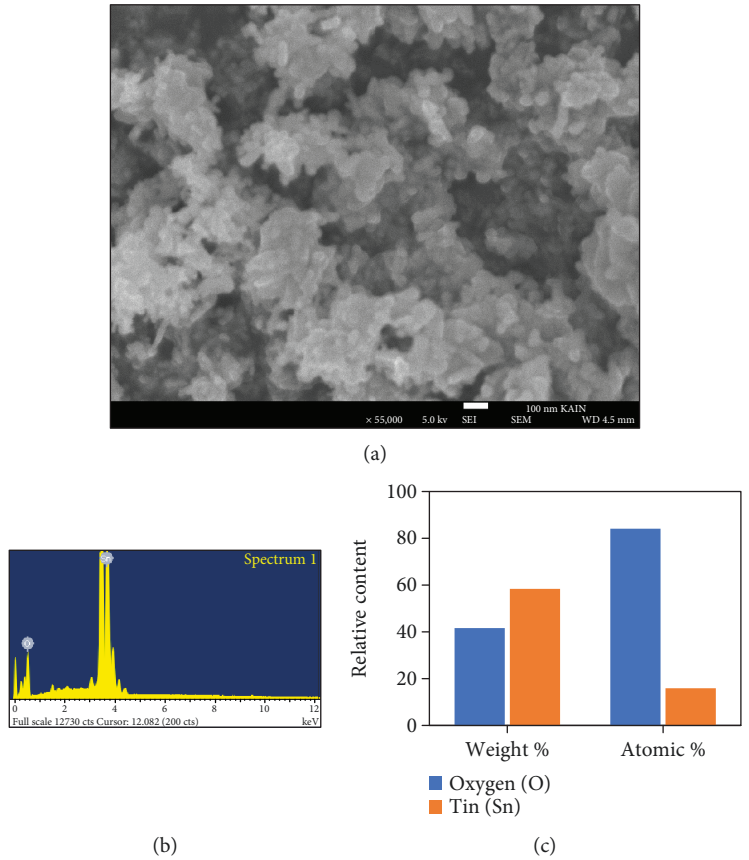

Figure 4: (a) Scanning electron micrograph of TONFs, (b) EDX profile, and (c) relative composition.

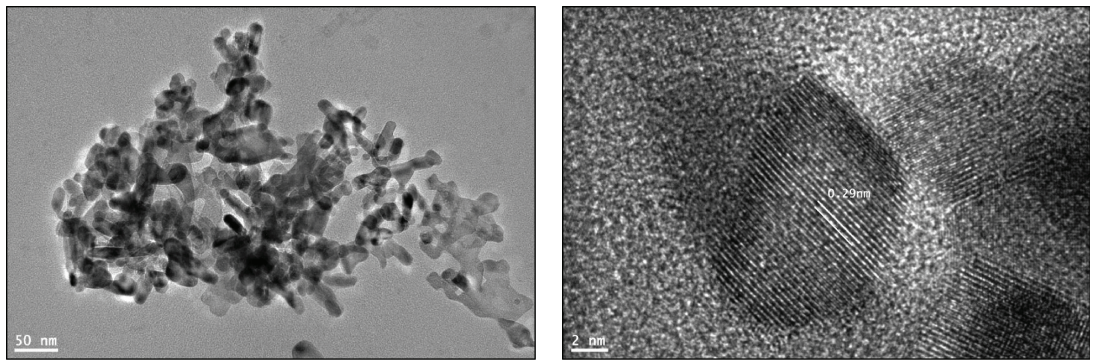

Figure 5: Transmission electron micrograph of TONFs.

dependent manner, and a significant drop in the violacein content was recorded at all tested concentrations. At 2 μg/ml concentration, TONFs decreased violacein production by 29% as compared to untreated control ($p \leq 0.05$). Similarly, with increasing concentration, gradual reduction in violacein was also observed to a maximum of 74% at a concentration of 16 μg/ml (Figure 7).

The results of violacein inhibition assay are comparable with those of Wagh et al. [46], who observed an 80% decrease in violacein production at 4 mg/ml. In another study, Singh et al. [47] reported 100% inhibition of violacein after treatment with mycofabricated silver nanoparticles.

3.6.2. Virulence Functions in P. aeruginosa PAO1. During infection, the production of virulence factors like elastase, protease, and pyocyanin invades and damages host tissue and leads to dissemination, leading to systemic spread of the pathogen [48]. Thus, QS-dependent production of virulence factors like elastase, protease, alginate, and pyocyanin was investigated to assess the effect of TONFs on virulence.

Elastase is a metalloprotease that facilitates the invasion and colonization of infection-causing bacteria by damaging host cell tissues. Proteases of bacteria hydrolyze a variety of host proteins and play a key role in host colonization [49]. When *P. aeruginosa* PAO1 was cultivated in the presence

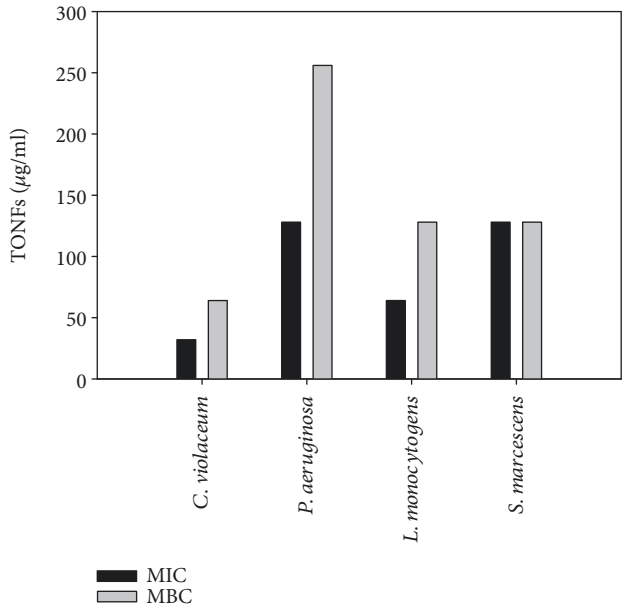

Figure 6: MIC and MBC values in μg/ml of TONFs against test pathogens.

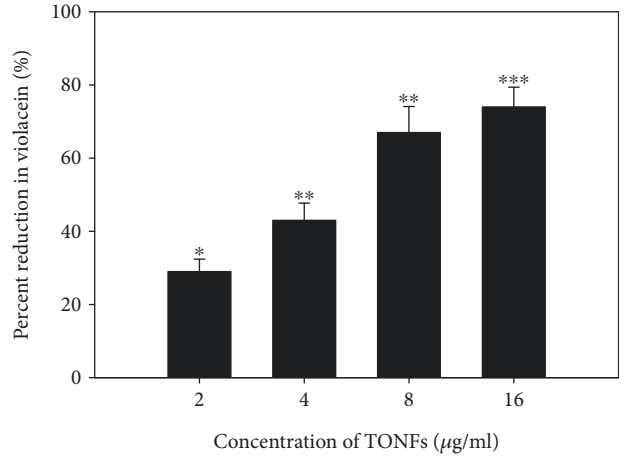

Figure 7: Effect of sub-MICs of TONFs on violacein production by *C. violaceum* 12472. $^{*}p \leq 0.05$ and $^{**}p \leq 0.005$.

of sub-MICs of TONFs, elastase activity was suppressed significantly to 59% and protease production was reduced up to 64% as compared to untreated control (Figure 8). Prateeksha et al. [50] reported a comparable decrease in elastase (52%) and protease (60%) after treatment with sub-MICs of selenium nanovectors.

QS regulates the production of a blue pigment called pyocyanin in *P. aeruginosa*. The role of pyocyanin in pathogenesis is well-known as it impairs the neutrophil-mediated defense system of the host [51]. Synthesized TONFs at subinhibitory concentrations reduced the pyocyanin production substantially (Figure 8). A maximum reduction of 61% was recorded at the highest tested concentration, i.e., 64 μg/ml, while a 22, 31, and 47% decrease was observed at 8, 16, and

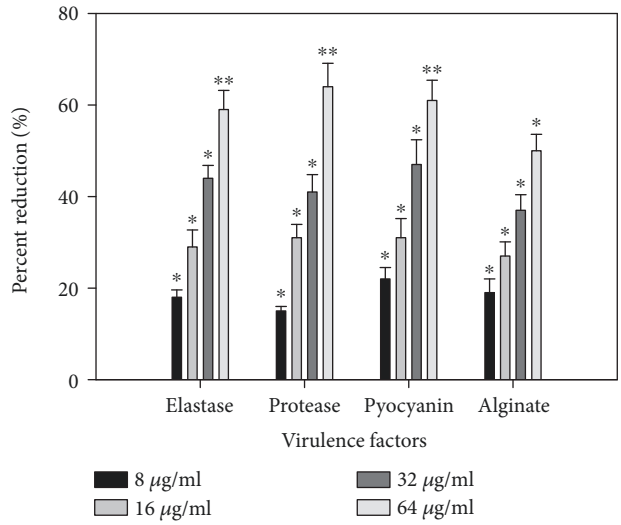

Figure 8: Effect of sub-MICs of TONFs on virulence factor production in *P. aeruginosa*. All of the data are presented as mean ± standard deviation. $^{*}p \leq 0.05$, $^{**}p \leq 0.005$, and $^{***}p \leq 0.001$.

32 μg/ml concentrations, respectively. Our observations on pyocyanin reduction find support from the reports on zinc nanoparticles [52] and silver nanoparticles [47].

Alginate is a major component of the exopolysaccharide matrix that surrounds the biofilm and confers resistance to bacteria against antimicrobials [27]. Therefore, any interference with alginate production is bound to reduce the rate of resistance among bacteria and make them more susceptible to antibacterial drugs. We observed that alginate production decreased with increase in concentration of TONFs. Alginate production was impaired by 19-50% at concentrations ranging from 8 to 64 μg/ml (Figure 8). Our results are in accordance with observations on green synthesized zinc oxide particles that arrested alginate production by 34-74% at tested sub-MICs [53].

3.6.3. Prodigiosin Inhibition in S. marcescens. Prodigiosin is a QS-regulated virulence function of *S. marcescens* and plays a vital role in the pathogenicity of the pathogen. A concentration-dependent decrease in prodigiosin production was recorded at sub-MICs ranging from 8 to 64 μg/ml (Figure 9). Prodigiosin was reduced maximally by 54% at 64 μg/ml concentration, while at the lowest tested concentration (8 μg/ml) its production decreased by 21%. This drop in prodigiosin production by *S. marcescens* was found to be significant at all tested concentrations ($p \leq 0.05$). Al-Shabib et al. [53] demonstrated 60% reduction in prodigiosin at 50 μg/ml concentration of zinc oxide nanoparticles. This finding corresponds to our results on prodigiosin reduction.

3.7. Effect of TONFs on Biofilm Formation. Biofilm formation in many bacteria is regulated by quorum sensing (QS). Bacteria residing in biofilm mode are surrounded by a layer of exopolysaccharides that functions as a protective sheath against environmental stress and host defense, leading to increased resistance to antimicrobials [48, 54]. Biofilm formation is considered as an important characteristic

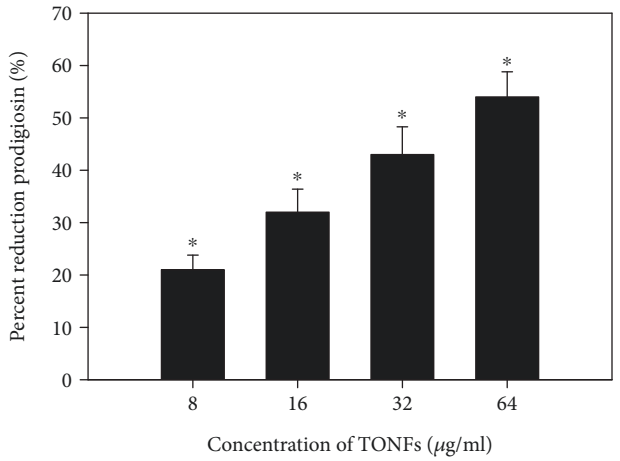

Figure 9: Effect of sub-MICs of TONFs on prodigiosin production in *S. marcescens*. All of the data are presented as mean ± standard deviation. $^{*}p \leq 0.05$ and $^{**}p \leq 0.005$.

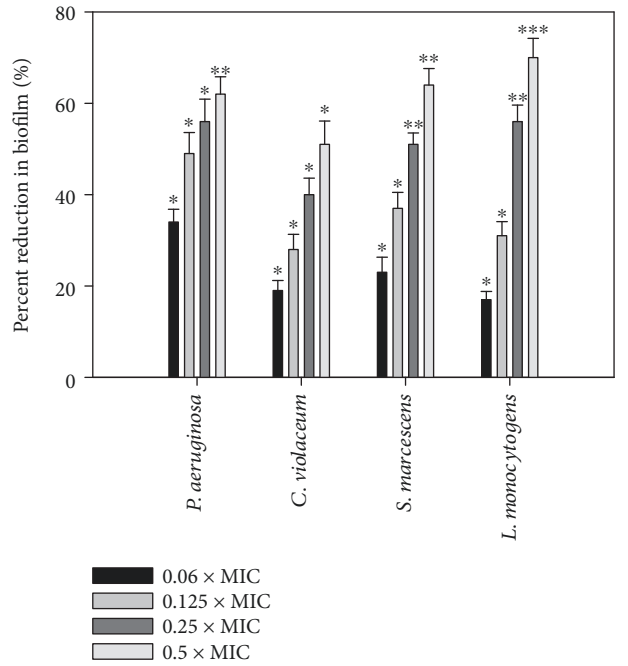

Figure 10: Effect of sub-MICs of TONFs on biofilm formation in test pathogens. All of the data are presented as mean ± standard deviation. $^{*}p \leq 0.05$, $^{**}p \leq 0.005$, and $^{***}p \leq 0.001$.

contributing to the virulence of pathogenic bacteria. Hence, sub-MICs of TONFs were assessed for their potential antibiofilm activity against test pathogens.

Microtitre plate assay for quantification of biofilm demonstrated a decrease in the biofilm formation capabilities of all pathogens after treatment with sub-MICs of TONFs as depicted in Figure 10. A concentration-dependent drop in biofilm formation was recorded for all tested pathogens at their respective sub-MICs. A maximum reduction of 62%, 51%, 64%, and 70% in the biofilm forming ability of *P. aeruginosa* PAO1, *C. violaceum* 12472, *S. marcescens*, and *L. monocytogenes* was observed over untreated control, respectively.

To validate the results of the biofilm inhibition assay, TONF-treated and untreated biofilm architecture was visualized using a confocal laser scanning microscope (CLSM). CLSM images of biofilm formation in test bacteria grown in the presence ($0.5 \times$MIC) and absence of TONFs are illustrated in Figure 11. It is quite evident from the images that biofilm formation was arrested substantially after the addition of tin nanoflowers. The untreated control showed thick aggregation of cells in all pathogens whereas TONF-treated bacteria showed disturbed architecture of microcolonies. A similar dose-dependent reduction of biofilm in pathogenic bacteria has been described with silver nanoparticles [45, 55], zinc oxide nanoparticles [52, 53], iron oxide nanoparticles [56], and copper oxide nanoparticles [57].

3.8. Effect on EPS and Swarming Motility. Exopolysaccharides and motility are vital in biofilm formation as the former is indispensable for the biofilm architecture and protects the biofilm for the action of antibiotics while the latter is responsible for the initial adhesion of pathogens to the surface [7]. Sub-MICs of TONFs demonstrated a significant reduction in EPS in all pathogens. EPS production was reduced by 48%, 55%, 41%, and 62% in PAO1, *C. violaceum* 12472, *S. marcescens*, and *L. monocytogenes*, respectively (Figure 12). A similar arrest in swarming migration was also observed at respective $0.5 \times$MIC of synthesized tin nanoflowers against all test pathogens. The diameter of swarm decreased by 66% and 58% in PAO1 and *S. marcescens*, respectively, at 64 μg/ml concentration, while at 16 μg/ml concentration motility was impaired by 62% in *C. violaceum* 12472. Motility of *L. monocytogenes* was also affected significantly, and a 61% drop was recorded at 32 μg/ml concentration as compared to untreated control (Figure 12). Our findings on EPS and motility inhibition corroborate well with the results obtained on reduced biofilm formation among test pathogens after treatment with synthesized TONFs. Since it is well documented that EPS and swarming motility are essential for the development and maturation of biofilms, interference with EPS and motility is bound to reduce biofilm formation.

3.9. Effect on Cell Surface Hydrophobicity (CSH). Cell surface hydrophobicity is also an important factor in the development of biofilm as it is the measure of the adhesion ability of the pathogen to the surface. Adhesion is the first step in biofilm development and is responsible for the subsequent infections and food spoilage in medical settings and the food industry, respectively. Since there is a positive correlation between hydrophobicity and adhesion, CSH is considered as a good indicator of the adhesion ability of the pathogen [54]. In the present investigation, CSH was reduced by 71%, 57%, 73%, and 64% in PAO1, *C. violaceum* 12472, *S. marcescens*, and *L. monocytogenes*, respectively, at respective $0.5 \times$MIC (Figure 12). Observations of the CSH assay clearly demonstrate that the synthesized tin nanoflowers inhibit the bacterial biofilm during the initial stages by impairing the adhesion ability of the pathogen to the surface.

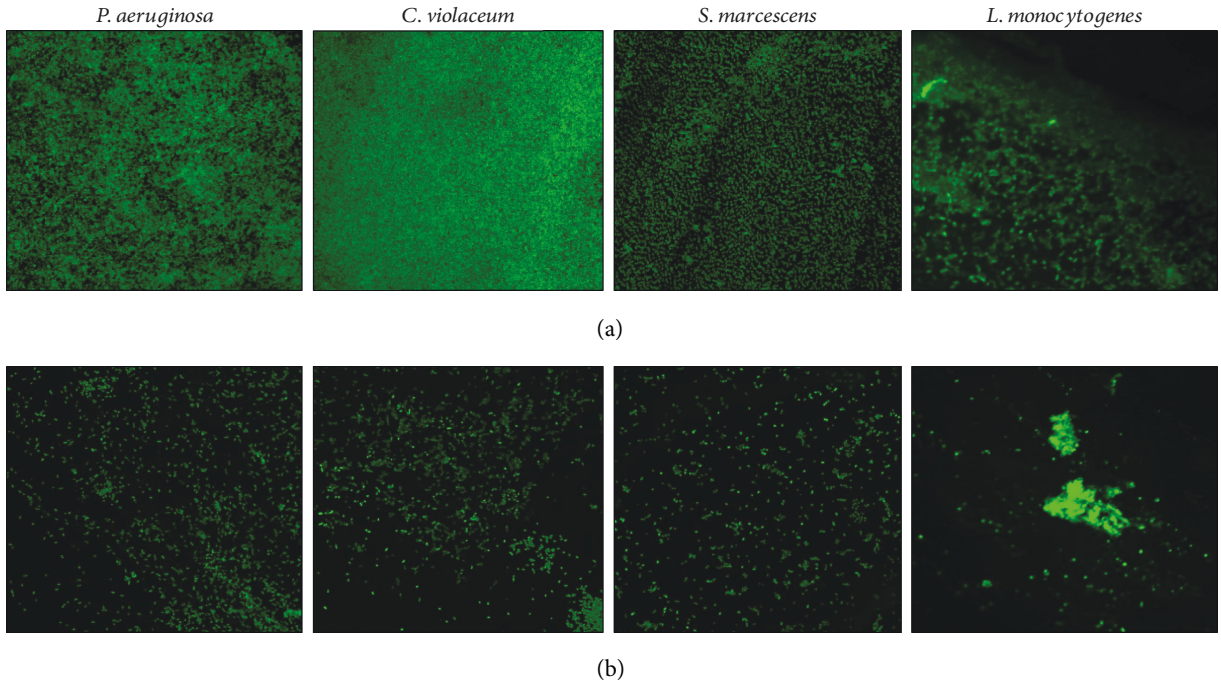

Figure 11: Visualization of biofilm inhibition using a confocal laser scanning microscope (CLSM). (a) Untreated control and (b) treatment with 0.5 × MIC of TONFs.

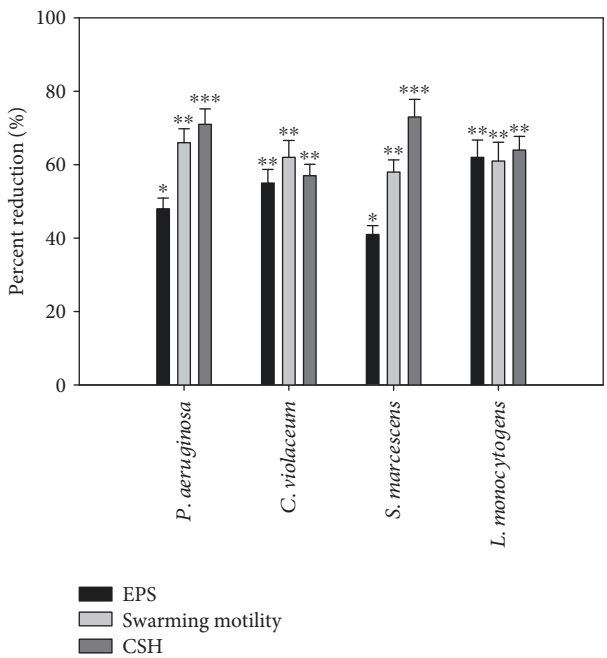

Figure 12: Effect of 0.5 × MICs of TONFs on swarming motility, EPS production, and cell surface hydrophobicity (CSH) of *P. aeruginosa*, *C. violaceum*, *S. marcescens*, and *L. monocytogenes*. All of the data are presented as mean ± standard deviation. $^{*}p \leq 0.05$, $^{**}p \leq 0.005$, and $^{***}p \leq 0.001$.

3.10. Eradication of Preformed Biofilms. Bacteria growing in planktonic mode are susceptible to antibiotics and disinfectants, but the susceptibility decreases several folds when these bacteria form biofilms [58]. Therefore, eradication preformed by biofilms by chemical agents is difficult in both healthcare and the food industry. In the present study, 0.5 × MICs of TONFs were tested for their ability to eradicate preformed biofilms of the test pathogens (Figure 13). Results showed that at 64 μg/ml, 24 h old biofilm of *P. aeruginosa* and *S. marcescens* was eradicated by 45 and 51%. For *C. violaceum*, 38% of the preformed biofilm was removed upon addition of 16 μg/ml while 64% of the *L. monocytogenes* biofilm was removed after treatment with 32 μg/ml concentration of TONFs. These findings suggest that the synthesized tin nanoflowers crossed the EPS matrix and successfully penetrated the biofilm, resulting in significant obliteration of the preformed biofilm in all tested pathogens. This is probably the first report on the eradication of preformed biofilm by tin oxide nanoparticles. However, similar results on biofilm eradication by silver nanoparticles have been reported against both Gram-negative and Gram-positive pathogens [34, 45].

4. Conclusions

Monophasic tin dioxide nanoflowers assembled by rod-like nanostructures were prepared by coprecipitation method without using any surfactants or templates. The study is significant as it demonstrated broad-spectrum inhibition of QS-regulated virulence and biofilm in pathogenic bacteria. Synthesized nanoflowers also exhibited significant eradication of the preformed biofilms. This is probably the first report on the interference of QS and biofilm inhibition using tin oxide nanoparticles. These findings suggest that synthesized TONFs could be exploited in the food industry and clinical settings for the removal of preformed biofilms. Based

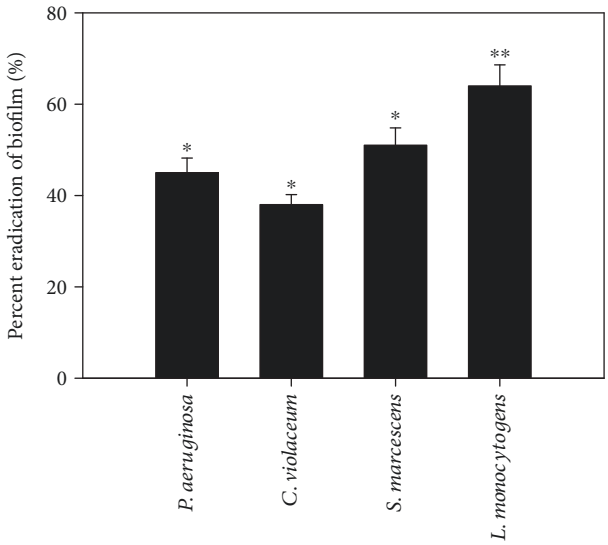

Figure 13: Eradication on 24 h preformed biofilm by sub-MICs of TONFs. All of the data are presented as mean ± standard deviation. $^{*}p \leq 0.05$, $^{**}p \leq 0.005$, and $^{***}p \leq 0.001$.

on all the observations, we can conclude that the biological activity demonstrated by TONFs will possibly help in preventing food spoilage and fighting drug-resistant infections.

Data Availability

Data can be provided after the publication of this article. The data used to support the findings of this study are currently under embargo while the research findings are commercialized. Requests for data, [6/12 months] after publication of this article, will be considered by the corresponding author [EA: updated on 7-Sep 2018].

Conflicts of Interest

The authors declare that they have no conflicts of interest.

Acknowledgments

The authors extend their appreciation to Deanship of Scientific Research at King Saud University for funding this work through Research Group no. RGP-1439-014.

References

[1] M. V. Alvarez, M. R. Moreira, and A. Ponce, "Antiquorum sensing and antimicrobial activity of natural agents with potential use in food," *Journal of Food Safety*, vol. 32, no. 3, pp. 379–387, 2012.

[2] K. Naik and M. Kowshik, "Anti-quorum sensing activity of AgCl-TiO2 nanoparticles with potential use as active food packaging material," *Journal of Applied Microbiology*, vol. 117, no. 4, pp. 972–983, 2014.

[3] A. Eberhard, A. L. Burlingame, C. Eberhard, G. L. Kenyon, K. H. Nealson, and N. J. Oppenheimer, "Structural identification of autoinducer of Photobacterium fischeri luciferase," *The Biochemist*, vol. 20, no. 9, pp. 2444–2449, 1981.

[4] R. B. Raffa, J. R. Iannuzzo, D. R. Levine et al., "Bacterial communication ("quorum sensing") via ligands and receptors: a novel pharmacologic target for the design of antibiotic drugs," *The Journal of Pharmacology and Experimental Therapeutics*, vol. 312, no. 2, pp. 417–423, 2005.

[5] M. Rasch, J. B. Andersen, K. F. Nielsen et al., "Involvement of bacterial quorum-sensing signals in spoilage of bean sprouts," *Applied and Environmental Microbiology*, vol. 71, no. 6, pp. 3321–3330, 2005.

[6] K. Sauer, A. K. Camper, G. D. Ehrlich, J. W. Costerton, and D. G. Davies, "Pseudomonas aeruginosa displays multiple phenotypes during development as a biofilm," *Journal of Bacteriology*, vol. 184, no. 4, pp. 1140–1154, 2002.

[7] I. A. S. V. Packiavathy, P. Agilandeswari, K. S. Musthafa, S. K. Pandian, and A. V. Ravi, "Antibiofilm and quorum sensing inhibitory potential of *Cuminum cyminum* and its secondary metabolite methyl eugenol against Gram negative bacterial pathogens," *Food Research International*, vol. 45, no. 1, pp. 85–92, 2012.

[8] M. M. Janus, B. J. F. Keijser, F. J. Bikker, R. A. M. Exterkate, W. Crielaard, and B. P. Krom, "*In vitro* phenotypic differentiation towards commensal and pathogenic oral biofilms," *Biofouling*, vol. 31, no. 6, pp. 503–510, 2015.

[9] M. E. Shirtliff, J. T. Mader, and A. K. Camper, "Molecular interactions in biofilms," *Chemistry & Biology*, vol. 9, no. 8, pp. 859–871, 2002.

[10] R. M. Corrigan and A. Gründling, "Cyclic di-AMP: another second messenger enters the fray," *Nature Reviews. Microbiology*, vol. 11, no. 8, pp. 513–524, 2013.

[11] K. K. Jefferson, "What drives bacteria to produce a biofilm?," *FEMS Microbiology Letters*, vol. 236, no. 2, pp. 163–173, 2004.

[12] P. N. Skandamis and G. J. E. Nychas, "Quorum sensing in the context of food microbiology," *Applied and Environmental Microbiology*, vol. 78, no. 16, pp. 5473–5482, 2012.

[13] V. C. Kalia, "Quorum sensing inhibitors: an overview," *Biotechnology Advances*, vol. 31, no. 2, pp. 224–245, 2013.

[14] T. Persson, M. Givskov, and J. Nielsen, "Quorum sensing inhibition: targeting chemical communication in gram-negative bacteria," *Current Medicinal Chemistry*, vol. 12, no. 26, pp. 3103–3115, 2005.

[15] M. Hentzer and M. Givskov, "Pharmacological inhibition of quorum sensing for the treatment of chronic bacterial infections," *The Journal of Clinical Investigation*, vol. 112, no. 9, pp. 1300–1307, 2003.

[16] A. Emamifar, "Applications of antimicrobial polymer nanocomposites in food packaging," in *Advances in Nanocomposite Technology*, A. Hashim, Ed., pp. 299–318, InTech, Rijeka, Croatia, 2011.

[17] C. Silvestre, D. Duraccio, and S. Cimmino, "Food packaging based on polymer nanomaterials," *Progress in Polymer Science*, vol. 36, no. 12, pp. 1766–1782, 2011.

[18] A. N. Sahu, "Nanotechnology in herbal medicines and cosmetics," *International journal of Research in Ayurveda & Pharmacy*, vol. 4, no. 3, pp. 472–474, 2013.

[19] M. F. Khan, A. H. Ansari, M. Hameedullah et al., "Sol-gel synthesis of thorn-like ZnO nanoparticles endorsing mechanical stirring effect and their antimicrobial activities: potential role as nano-antibiotics," *Scientific Reports*, vol. 6, no. 1, article 27689, 2016.

[20] M. R. Vaezi and S. K. Sadrnezhaad, "Gas sensing behavior of nanostructured sensors based on tin oxide synthesized with

different methods," *Materials Science and Engineering: B*, vol. 140, no. 1-2, pp. 73–80, 2007.

[21] V. K. Vidhu and D. Philip, "Biogenic synthesis of SnO_2 nanoparticles: evaluation of antibacterial and antioxidant activities," *Spectrochimica Acta. Part A, Molecular and Biomolecular Spectroscopy*, vol. 134, pp. 372–379, 2015.

[22] M. Meena Kumari and D. Philip, "Synthesis of biogenic SnO_2 nanoparticles and evaluation of thermal, rheological antibacterial and antioxidant activities," *Powder Technology*, vol. 270, pp. 312–319, 2015.

[23] N. M. Al-Hada, H. M. Kamari, A. A. Baqer, A. H. Shaari, and E. Saion, "Thermal calcination-based production of SnO_2 nanopowder: an analysis of SnO_2 nanoparticle characteristics and antibacterial activities," *Nanomaterials*, vol. 8, no. 4, p. 250, 2018.

[24] A. Klančnik, S. Piskernik, B. Jeršek, and S. S. Mozina, "Evaluation of diffusion and dilution methods to determine the antibacterial activity of plant extracts," *Journal of Microbiological Methods*, vol. 81, no. 2, pp. 121–126, 2010.

[25] F. M. Husain, I. Ahmad, M. H. Baig et al., "Broad-spectrum inhibition of AHL-regulated virulence factors and biofilms by sub-inhibitory concentrations of ceftazidime," *RSC Advances*, vol. 6, no. 33, pp. 27952–27962, 2016.

[26] F. M. Husain, I. Ahmad, M. Asif, and Q. Tahseen, "Influence of clove oil on certain quorum sensing regulated functions and biofilm of *Pseudomonas aeruginosa* and *Aeromonas hydrophila*," *Journal of Biosciences*, vol. 38, no. 5, pp. 835–844, 2013.

[27] V. Gopu, C. K. Meena, and P. H. Shetty, "Quercetin influences quorum sensing in food borne bacteria: *in-vitro* and *in-silico* evidence," *PLoS One*, vol. 10, no. 8, article e0134684, 2015.

[28] T. Morohoshi, T. Shiono, K. Takidouchi et al., "Inhibition of quorum sensing in *Serratia marcescens* AS-1 by synthetic analogs of *N-acylhomoserine* lactone," *Applied and Environmental Microbiology*, vol. 73, no. 20, pp. 6339–6344, 2007.

[29] K. Kalishwaralal, S. BarathManiKanth, S. R. K. Pandian, V. Deepak, and S. Gurunathan, "Silver nanoparticles impede the biofilm formation by *Pseudomonas aeruginosa* and *Staphylococcus epidermidis*," *Colloids and Surfaces B: Biointerfaces*, vol. 79, no. 2, pp. 340–344, 2010.

[30] A. L. Huston, B. Methe, and J. W. Deming, "Purification, characterization and sequencing of an extracellular cold-active aminopeptidase produced by marine psychrophile *Colwellia psychrerythraea* strain 34H," *Applied and Environmental Microbiology*, vol. 70, no. 6, pp. 3321–3328, 2004.

[31] M. DuBois, K. A. Gilles, J. K. Hamilton, P. A. Rebers, and F. Smith, "Use of phenol reagent for the determination of total sugar," *Analytical Chemistry*, vol. 28, pp. 350–356, 1956.

[32] F. M. Husain and I. Ahmad, "Doxycycline interferes with quorum sensing-mediated virulence factors and biofilm formation in Gram-negative bacteria," *World Journal of Microbiology and Biotechnology*, vol. 29, no. 6, pp. 949–957, 2013.

[33] D. Viszwapriya, U. Prithika, S. Deebika, K. Balamurugan, and S. K. Pandian, "*In vitro* and *in vivo* antibiofilm potential of 2,4-di-*tert*-butylphenol from seaweed surface associated bacterium *Bacillus subtilis* against group a streptococcus," *Microbiological Research*, vol. 191, pp. 19–31, 2016.

[34] S. Gaidhani, R. Singh, D. Singh et al., "Biofilm disruption activity of silver nanoparticles synthesized by *Acinetobacter calcoaceticus* PUCM 1005," *Materials Letters*, vol. 108, pp. 324–327, 2013.

[35] S. Tazikeh, A. Akbari, A. Talebi, and E. Talebi, "Synthesis and characterization of tin oxide nanoparticles via the co-precipitation method," *Materials Science-Poland*, vol. 32, no. 1, pp. 98–101, 2014.

[36] L. M. Fang, X. T. Zu, Z. J. Li et al., "Synthesis and characteristics of Fe^{3+}-doped SnO_2 nanoparticles *via* sol–gel-calcination or sol–gel-hydrothermal route," *Journal of Alloys and Compounds*, vol. 454, no. 1-2, pp. 261–267, 2008.

[37] P. S. Patil, R. K. Kawar, T. Seth, D. P. Amalnerkar, and P. S. Chigare, "Effect of substrate temperature on structural, electrical and optical properties of sprayed tin oxide (SnO_2) thin films," *Ceramics International*, vol. 29, no. 7, pp. 725–734, 2003.

[38] W. Xia, H. Wang, X. Zeng et al., "High-efficiency photocatalytic activity of type II SnO/Sn_3O_4 heterostructures via interfacial charge transfer," *CrystEngComm*, vol. 16, no. 30, pp. 6841–6847, 2014.

[39] A. Azam, S. Habib, N. Salah, and F. Ahmed, "Microwave-assisted synthesis of SnO_2 nanorods for oxygen gas sensing at room temperature," *International Journal of Nanomedicine*, vol. 8, no. 1, pp. 3875–3882, 2013.

[40] A. D. Bhagwat, S. S. Sawant, B. G. Ankamwar, and C. M. Mahajan, "Synthesis of nanostructured tin oxide (SnO_2) powders and thin films by sol-gel method," *Journal of Nano- and Electronic Physics*, vol. 7, no. 4, article 04037, 2015.

[41] L. Jiang, G. Sun, Z. Zhou et al., "Size-controllable synthesis of monodispersed SnO_2 nanoparticles and application in electrocatalysts," *The Journal of Physical Chemistry. B*, vol. 109, no. 18, pp. 8774–8778, 2005.

[42] M. Jeyaraj, S. Varadan, K. J. P. Anthony, M. Murugan, A. Raja, and S. Gurunathan, "Antimicrobial and anticoagulation activity of silver nanoparticles synthesized from the culture supernatant of *Pseudomonas aeruginosa*," *Journal of Industrial and Engineering Chemistry*, vol. 19, no. 4, pp. 1299–1303, 2013.

[43] S. Das, S. Kar, and S. Chaudhuri, "Optical properties of SnO_2 nanoparticles and nanorods synthesized by solvothermal process," *Journal of Applied Physics*, vol. 99, no. 11, article 114303, 2006.

[44] N. A. Begum, S. Mondal, S. Basu, R. A. Laskar, and D. Mandal, "Biogenic synthesis of Au and Ag nanoparticles using aqueous solutions of black tea leaf extracts," *Colloids and Surfaces. B, Biointerfaces*, vol. 71, no. 1, pp. 113–118, 2009.

[45] F. A. Qais, Samreen, and I. Ahmad, "Broad-spectrum inhibitory effect of green synthesised silver nanoparticles from Withania somnifera (L.) on microbial growth, biofilm and respiration: a putative mechanistic approach," *IET Nanobiotechnology*, vol. 12, no. 3, pp. 325–335, 2018.

[46] M. S. Wagh, R. H. Patil, D. K. Thombre, M. V. Kulkarni, W. N. Gade, and B. B. Kale, "Evaluation of anti-quorum sensing activity of silver nanowires," *Applied Microbiology and Biotechnology*, vol. 97, no. 8, pp. 3593–3601, 2013.

[47] B. R. Singh, B. N. Singh, A. Singh, W. Khan, A. H. Naqvi, and H. B. Singh, "Mycofabricated biosilver nanoparticles interrupt Pseudomonas aeruginosa quorum sensing systems," *Scientific Reports*, vol. 5, no. 1, article 13719, 2015.

[48] S. Wagner, R. Sommer, S. Hinsberger et al., "Novel strategies for the treatment of *Pseudomonas aeruginosa* infections," *Journal of Medicinal Chemistry*, vol. 59, no. 13, pp. 5929–5969, 2016.

[49] S. Sarabhai, P. Sharma, and N. Capalash, "Ellagic acid derivatives from *Terminalia chebula* Retz. downregulate the

expression of quorum sensing genes to attenuate *Pseudomonas aeruginosa* PAO1 virulence," *PLoS One*, vol. 8, no. 1, article e53441, 2013.

[50] Prateeksha, B. R. Singh, M. Shoeb et al., "Scaffold of selenium nanovectors and honey phytochemicals for inhibition of *Pseudomonas aeruginosa* quorum sensing and biofilm formation," *Frontiers in Cellular and Infection Microbiology*, vol. 7, p. 93, 2017.

[51] J. L. Fothergill, S. Panagea, C. A. Hart, M. J. Walshaw, T. L. Pitt, and C. Winstanley, "Widespread pyocyanin overproduction among isolates of a cystic fibrosis epidemic strain," *BMC Microbiology*, vol. 7, no. 1, p. 45, 2007.

[52] N. A. Al-Shabib, F. M. Husain, F. Ahmed et al., "Biogenic synthesis of zinc oxide nanostructures from *Nigella sativa* seed: prospective role as food packaging material inhibiting broad-spectrum quorum sensing and biofilm," *Scientific Reports*, vol. 6, no. 1, article 36761, 2016.

[53] N. A. Al-Shabib, F. M. Husain, I. Hassan et al., "Biofabrication of zinc oxide nanoparticle from *Ochradenus baccatus* leaves: broad-spectrum antibiofilm activity, protein binding studies, and *in vivo* toxicity and stress studies," *Journal of Nanomaterials*, vol. 2018, Article ID 8612158, 14 pages, 2018.

[54] A. Silva-Dias, I. M. Miranda, J. Branco, M. Monteiro-Soares, C. Pina-Vaz, and A. G. Rodrigues, "Adhesion biofilm formation, cell surface hydrophobicity, and antifungal planktonic susceptibility: relationship among *Candida* Spp," *Frontiers in Microbiology*, vol. 6, p. 205, 2015.

[55] S. Qayyum, M. Oves, and A. U. Khan, "Obliteration of bacterial growth and biofilm through ROS generation by facilely synthesized green silver nanoparticles," *PLoS One*, vol. 12, no. 8, article e0181363, 2017.

[56] P. Velusamy, S. Chia-Hung, A. Shritama, G. V. Kumar, V. Jeyanthi, and K. Pandian, "Synthesis of oleic acid coated iron oxide nanoparticles and its role in anti-biofilm activity against clinical isolates of bacterial pathogens," *Journal of the Taiwan Institute of Chemical Engineers*, vol. 59, pp. 450–456, 2016.

[57] M. Agarwala, B. Choudhury, and R. N. S. Yadav, "Comparative study of antibiofilm activity of copper oxide and iron oxide nanoparticles against multidrug resistant biofilm forming uropathogens," *Indian Journal of Microbiology*, vol. 54, no. 3, pp. 365–368, 2014.

[58] A. Bridier, R. Briandet, V. Thomas, and F. Dubois-Brissonnet, "Resistance of bacterial biofilms to disinfectants: a review," *Biofouling*, vol. 27, no. 9, pp. 1017–1032, 2011.